Title: Postnatal Enrichment Corrects Deficits in Perineuronal Net Formation and Reversal Learning in Adult Mice Exposed to Early Adversity

Running title: Enrichment Corrects Cognitive Deficits in LB Mice

Authors:

Sumit Jamwal[1]
Rafiad Islam[1]
Zoe MacDowell Kaswan[1]
Sahabuddin Ahmed[1]
Christian Bowers[1]
Lauryn Giuliano[1]
Arie Kaffman[1*]

Affiliations

1. Department of Psychiatry, Yale University School of Medicine, 300 George Street, Suite 901, New Haven CT, 06511, USA.

* Corresponding author: Arie Kaffman, 300 George Street, Suite 901, New Haven CT, 06511, USA. email: arie.kaffman@yale.edu, phone: 203-785-6657

Key words: Limited bedding and nesting, early life adversity (ELA), Enrichment, reversal learning, orbitofrontal cortex, cognitive flexibility, perineuronal nets (PNN), parvalbumin cells, excitatory-inhibitory balance.

Word count: manuscript: 6142, abstract: 249

Abstract

Childhood neglect is associated with cortical thinning, hyperactivity, and deficits in cognitive flexibility that are difficult to reverse later in life. Despite being the most prevalent form of early adversity, little is currently understood about the mechanisms responsible for these neurodevelopmental abnormalities, and no animal models have yet replicated key structural and behavioral features of childhood neglect/deprivation. To address these gaps, we have recently demonstrated that mice exposed to impoverished conditions, specifically limited bedding (LB), exhibit behavioral and structural changes that resemble those observed in adolescents who have experienced severe neglect. Here, we show that LB leads to long-term deficits in reversal learning, which can be fully reversed by briefly exposing LB pups to enrichment (toys) in their home cage from postnatal days 14 to 25. Reversal learning failed to induce normal c-fos activation in the orbitofrontal cortex (OFC) of LB mice, a deficit that was normalized by early enrichment. Additionally, LB decreased the density of parvalbumin-positive cells surrounded by perineuronal nets (PV+PNN+) and increased the ratio of glutamatergic to inhibitory synapse densities in the OFC, deficits that were also reversed by enrichment. Degradation of PNN in the OFC of adult mice impaired reversal learning, reduced c-fos activation, and increased the ratio of glutamatergic to inhibitory synapse densities in the OFC to levels comparable to those observed in LB mice. Collectively, our findings suggest that postnatal deprivation and enrichment impact the formation of PV+PNN+ cells in the OFC, a developmental process that is essential for cognitive flexibility in adulthood.

Introduction

The Child Maltreatment Report issued by the Department of Health and Human Services documented 600,000 cases of early life adversity (ELA) in 2021 alone[1]. The majority of these cases were attributed to neglect (76%), followed by physical abuse (16%) and sexual abuse (10%). Childhood neglect increases the risk of various psychopathologies, including anxiety, depression, attention-deficit/hyperactivity disorder (ADHD), as well as social and cognitive deficits[2-5]. The cognitive impairments observed in neglected children, or in those who have been institutionalized and exposed to severe deprivation early in life, include reduced IQ and impaired executive functions in areas such as working memory and cognitive flexibility[2, 5]. Cognitive deficits in children exposed to neglect and deprivation are more pronounced than those seen in other forms of ELA, such as physical or sexual abuse, and are highly correlated with the duration of deprivation/neglect and the extent of cortical thinning — another unique structural abnormality observed in childhood neglect and deprivation[2, 4, 5].

Cognitive flexibility is essential for adaptability, which is the ability to effectively regulate thoughts, emotions, and behaviors when confronted with new and uncertain situations [6-8]. Adaptability is now recognized as a crucial personal resource for ensuring well-being, protecting against psychopathology, and successfully navigating challenges in areas such as school, work, and social interactions[6-9]. Consequently, abnormal adaptability may be a core deficit responsible for many of the negative outcomes observed in individuals exposed to neglect or deprivation[2, 10-12]. While early adoption and enrichment strategies have been shown to improve IQ, language development, reward learning, and white matter volume and integrity, they have not been effective in addressing cortical thinning or deficits in cognitive flexibility or adaptability[2, 4]. Abnormal orbitofrontal cortex (OFC) development and function may explain deficits in cognitive flexibility and adaptability because childhood neglect and deprivation impair OFC development[4, 13-17] and perturbation of OFC function causes deficits in cognitive flexibility and adaptability in humans and in animals[18].

Even though neglect is the most prevalent form of ELA, it is the least studied[1, 3, 19, 20], and no animal models have yet replicated the key structural and behavioral features associated with childhood deprivation and neglect[21]. Furthermore, existing enrichment research has primarily focused on adult animals[22], with only a few studies investigating the effects of early enrichment on cognitive and structural deficits induced by ELA[23-26]. To address these gaps, we recently demonstrated that adolescent mice exposed to extended impoverished conditions—characterized by limited bedding (LB) from birth to postnatal day 25 (P25) — exhibit significant cortical thinning and hyperactivity, resembling the effects observed in adolescents subjected to

severe neglect and deprivation[21]. Using the Barnes maze reversal learning task as a model for adaptability, we assessed the impact of LB and postnatal enrichment on task performance and OFC function in adult mice. The experimental design included a control condition (CTL), mice exposed to LB from P0-25, and mice exposed to LB from P0-25 but also provided with toys in their home cage from P14 until P25, a condition we termed LB + toys (LBT). Adult LB mice exhibited profound deficits in reversal learning, which were completely mitigated by postnatal enrichment. Early enrichment also normalized c-fos activation and the formation of perineuronal nets around parvalbumin-positive (PV+PNN+) cells in the OFC of adult mice previously exposed to LB. LB increased the ratio of putative excitatory to inhibitory synapses (E-I balance) in the OFC, an abnormality that was reversed with early enrichment. Degradation of PNN in the OFC of adult CTL mice led to deficits in reversal learning, reduced c-fos activation, and an increased E-I balance in the OFC to levels comparable to those observed in LB mice. Collectively, these findings reveal a novel role for PNN formation in the OFC as a critical developmental process that guides cognitive flexibility and adaptability in response to early deprivation and enrichment.

Methods

Animals

BALB/cByj mice (Stock # 001026, Jackson Laboratories) were kept on a standard 12:12 hr light-dark cycle (lights on at 7:00AM), with food provided *ad libitum*. Temperature and humidity were held constant (23 ± 1ºC and 43% ± 2). All studies were approved by the Institutional Animal Care and Use Committee (IACUC) at Yale University and were conducted in accordance with the recommendations of the NIH Guide for the Care and the Use of Laboratory Animals.

Postnatal Manipulations

The limited bedding (LB) procedure was performed as described previously[21, 27]. Briefly, breeding cages were set up using a 3:1 female to male harem in standard mouse Plexiglas cages with 2 cups corncob bedding and no nesting material. Visibly pregnant dams were transferred to ‘maternity cages’ containing 2 cups corncob bedding with no nesting material and 3 chow pellets on the floor. At birth (P0), litters were culled to 5–8 pups and randomized to either control (CTL), limited bedding (LB), or limited bedding plus toys (LBT). CTL litters were provided with 500 cc of corncob bedding, 15cc of soiled bedding from the birth cage, and one 5 × 5 cm nestlet from P0-25. LB and LBT litters were provided with 125 cc corncob, 15 cc of soiled bedding from the birth cage, and no nestlet from P0-25. Bedding was changed on P7, P14, and P21. LBT litters were maintained under the same conditions as LB mice, except that

they were provided with toys in their home cage from P14 until P25. These include one safe harbor (Cat# K3583, Lab Supplies), 3 glass marbles (Assorted-Classical-Colorful-Marbles, Amazon) and 2 wooden blocks (You & Me Block Chews for Small Animals, Cat# 2493929, Petco). See figure 1B-C. Mice were weaned on P26 and housed with 2-3 same-sex littermates per cage with 500cc of corncob bedding, no nesting material, and 2-3 chow pellets on the floor.

Behavioral testing

All behavioral tests were conducted between 9:00-13:00. No more than 3 mice per sex were tested from each litter, and all behavioral tests had at least 8 litters per sex and rearing group (the number of mice and litters for each study is available in the figure legends).

Open Field Test

Mice were allowed to explore a 50 × 50 cm arena (lux 60) for 5 min. Distance traveled and the time spent in the inner 15 cm area were measured using the Ethovision tracking system (Noldus Information Technology).

Barnes maze

The Barnes maze task was employed to evaluate spatial learning and reversal learning/adaptability. A 20-hole gray circular Barnes Maze (Cat# 3601, Maze Engineers) was utilized, featuring an overhead light (600 lux) at the center to motivate escape, along with three visual cues positioned on the walls surrounding the maze. During a single habituation trial, the mouse was placed in an opaque cylinder at the center of the maze. After 10 seconds, the cylinder was removed, allowing the mouse to search for the escape hole for 1 minute. Mice that did not locate the target hole within this time frame were gently guided into the escape box using a long, thin wooden rod. All mice were kept in the escape chamber for 1 minute before being returned to their home cage. During the acquisition phase (Days 1-4), mice were placed in an opaque box positioned in the center of the maze for 10 seconds, after which they were allowed to search for the escape box for 3 minutes. Mice that failed to find the target hole were guided to it and permitted to remain there for 1 minute. Each mouse underwent training twice daily with a 30-minute inter-trial interval. Following the acquisition phase, mice were tested for 90 seconds in a probe trial with the escape box removed (Day 5). After the probe test, the target hole was repositioned 180° from its original location, and mice were assessed for reversal learning (Days 6-9) using the same protocol as in the acquisition phase (e.g., 180 seconds per trial, 2 daily trials, 30-minute inter-trial interval). On day 10, mice were tested in the reversal

learning probe trial for 90 seconds. Between trials, the maze and holes were cleaned with 70% ethanol and randomly rotated to eliminate odor cues. Video tracking software (Ethovision XT, Noldus) was employed to calculate the latency to reach the target hole, and the time spent in the target quadrant. Learning indexes during the acquisition (Figures 1E & 4D) and reversal learning phases (Figures 1K & 4I) were calculated using mean escape latencies as follow: (first day – last day)/ (first day + last day).

Tissue Collection and Processing

Tissue for immunohistochemistry was collected 90 minutes after the reversal learning probe trial. Mice were anesthetized and transcardially perfused with an ice-cold PBS/heparin (50 u/ml) solution (Bio-Rad, Cat #1610780; Sigma, Cat# H3393), followed by 10% formalin (Polyscience, Cat# 08279-20). The brains were post-fixed for 1hr with 10% formalin at room temperature and then stored in PBS at 4°C until processed for immunohistochemistry.

Immunohistochemistry

Fifty-micron coronal sections were collected using a VT1000S vibratome (Leica) in 4 pools, each containing 3 slices, spanning the entire rostral-caudal axis of the orbitofrontal cortex. For perineuronal nets (PNN), parvalbumin (PV) and c-fos staining, one pool of slices was first washed (3 x15 min) with TBST (TBS with 0.5% Triton-X100) and then blocked for 2 hr. at room temperature using 5 % normal goat serum (NGS) (Cat# 005-000-12, Jackson Immuno Research laboratories) in TBST (American bio, CAS 9002-93-1). Sections were then incubated with WFA-biotinylated (1:200; Cat. #B-1355-2, Vector labs), guinea pig anti-PV^{+} antibodies (1:2000; Cat. #195004, Synaptic System), and rabbit anti-c-fos antibodies (1:3000, Cat. #2250S, Cell Signaling Technology) in TBST and 3 % NGS. After 48 hr incubation, sections were washed with TBST 0.5% (3 x15 min) and then incubated for 2 hr at room temperature with the following 2 μg/ml secondary antibodies: Alexa488-conjugated streptavidin (Cat. #016-540-084, Jackson ImmunoResearch), Alexa-555 goat anti-rabbit (1:400; Cat. #A21428, Invitrogen), and Alexa 633 goat anti-guinea pig (1:400; Cat. #A21105, Invitrogen). Slices were then washed with TBST (3 x15 min) and mounted on glass slides with VECTASHIELD Vibrance antifade mounting medium with DAPI (Cat# 1800, Vector laboratories).

To assess the density of putative glutamatergic and GABAergic functional synapses, sections were washed with TBST and blocked as described above. For glutamatergic synapse density, sections were stained overnight at 4°C with guinea pig anti-Vglut2 antibodies (1:700, Cat. #AB2251-I, EMD-Millipore), and mouse anti-PSD95 antibodies (1:100, Cat. #MAB1596,

Merck-Millipore). For GABAergic functional synapses, sections were stained overnight at 4°C with rabbit anti-VGAT antibodies (1:1000, Cat. #131002, Synaptic System), and mouse anti-Gephyrin (1:1000, Cat. #147011, Synaptic System). Sections were then washed with TBST (3 X 15 min) and incubated for 2 hrs at room temperature with the appropriate fluorescently labelled secondary antibodies: Alexa 555 goat anti-mouse (1:400, Cat. # A21422, Invitrogen), Alexa 633 goat anti-guinea pig (1:400, Cat. # A21105, Invitrogen), and Alexa 633 goat anti-rabbit (1:400, Cat. #A21071, Invitrogen). Sections were washed with TBST and mounted on glass slides with VECTASHIELD Vibrance antifade mounting medium with DAPI (Cat# 1800, Vector laboratories).

Microscopy and Image Analysis

To determine the total number of PNN-positive cells, PV-positive cells, and c-fos-positive cells, high-resolution (1024 x 1024) confocal Z stack images of the orbitofrontal cortex region were acquired using an Olympus FV-3000 microscope equipped with a 20X objective. Images were acquired at 0.30 µm intervals for a total thickness of 15-20 µm. The acquired images were deconvoluted and processed using Imaris version 10.1.1 (Oxford Instruments) equipped with artificial intelligence machine learning capabilities to reliably detect and count specific cell population using the following protocol. First, a 600 µm x 600 µm x10 µm region of interest was selected using the cropped 3D function with each channel adjusted using gaussian filter and background subtraction. PV+ cells were defined using the 'surface function' wizard box, with a surface of 1.99 µm and absolute intensity. PNN+ cells were defined using a 0.99 µm surface and a machine learning segmentation protocol that included a 0.3 µm slicer extended section and seed point 10 µm. The 'shortest distance to surface-surface PNN' filter was then used to count number of PNN+, PV+ cells, PNN+PV+, PNN-PV+, and PNN+PV- cells. The total number of c-fos+ cells was counted using the 'spot function' with a XY diameter of 10 µm and Z-axis elongation at 10 µm. Spots were selected based on the 'Quality' filter type with the center point and radius size set at 10. The total number of cells obtained from 4-6 pictures were averaged to determine the final count for each cell papulation.

To assess glutamatergic and GABAergic spine density, high-resolution (1024 x 1024), Z stack images of the OFC were acquired at 0.30 µm intervals for a total thickness of 15-20 µm using an Olympus FV-3000 microscope, 60X objective, and 2x digital zoom. The acquired images were deconvoluted and processed using the Imaris version 10.1.1 (Oxford Instruments) according to the following protocol. A 25 µm x 50 µm x10 µm region of interest was selected using the cropped 3D function with each channel adjusted using gaussian filter, automated

background subtraction, and gamma correction. A 3D reconstruction spots were created for each channel using the 'spot function' with an XY diameter of 0.2 µm and Z-axis elongation at 10 µm. Spots were selected based on the 'Quality' filter type with the center point and radius size set at 10. Finally, the 'shortest distance to spot-spot' filter was used to determine the density of presynaptic and postsynaptic puncta that were less than 0-250 nm apart and therefore considered putative functional synapses. The densities obtained from 4-6 images were averaged to determine the densities of VGlut2 puncta, PSD95 puncta, putative functional glutamatergic synapses, VGAT puncta, GEPHYRIN puncta, and putative GABAergic synapses in the OFC of each mouse. The E-I balance was calculated by dividing the densities of putative glutamatergic and GABAergic synapses in the OFC for each animal.

ChABC injections

P84 adult CTL male mice were administered Ethiqa XR (3.25 mg/kg), anesthetized with isoflurane (1-3%), and placed in a stereotaxic apparatus (Cat# 51725D, Stoelting) equipped with a nose cone (Cat #50264, Stoelting). A sagittal midline incision was made using a sterile technique and the skull drilled using a high-speed drill. Protease-free Chondroitinase ABC (ChABC; Sigma Aldrich, St. Louis, MO) was dissolved in saline solution containing 0.1% BSA (Cat# A3294, Sigma Aldrich, St. Louis, MO) to 50 U/ml of concentration and filtered through a 0.2-micron filter. For vehicle injections, saline 0.1% BSA was filtered as above. Initial characterization was done by injecting 1uL of ChABC (50 U/ml) into the right OFC and 1uL of vehicle injected into the left OFC (Figure S5). However, for studies reports in figures 4-6, 1 uL of ChABC (50 U/ml) or vehicle were injected into the OFC bilaterally at 0.2 µl/min with a 33-gauge needle using the following coordinates: anterior–posterior: +2.7, medial-lateral: ± 1, and dorsal-ventral: − 2.4, all in mm from bregma. The needle remained in place for 3 min before being slowly withdrawn over 2 min. The incision was closed with Vet Bond, and the mice were allowed to fully recover prior to being returned to their home cage.

Statistical Analysis

The data were carefully screened for inaccuracies, outliers, normality, and homogeneity of variance using SPSS (IBM Corp. version 26) and visualized with GraphPad Prism (iOS, version 10.0). Sample sizes were determined based on effect sizes obtained from preliminary studies, with alpha = 0.05, and a power > 0.8 and outliers removed if they were more than 2 standard deviations above or below the mean. Two-way ANOVA was used to assess the effects of rearing (CTL, LB, LBT), sex, and their interaction on exploration in the open field (Figure S1 A-

C), learning index (Figure 1 E & K), behavioral outcomes in the probe trial (Figure 1 F, G, L, M), cellular densities in the OFC (Figure 2 B-G), and synaptic densities in the OFC (Figure 3). Since similar outcomes were observed in males and females, significant rearing effects were further analyzed using Tukey's HSD post-hoc tests across the rearing conditions (e.g., CTL vs. LB, LB vs. LBT, and CTL vs. LBT). A repeated measures ANOVA (rmANOVA) was conducted to evaluate the effects of training days as a within-subject variable, with rearing and sex as between-subject variables, and the interaction among all three variables (Figure 1 D & J). Given that similar outcomes were noted in males and females, significant rearing effects were followed by Tukey's HSD post-hoc analyses as described above. Pearson correlation was utilized to examine the relationship between the number of PV+PNN+ cells, c-fos+ cells, and performance in the probe trial (Figure 2 H-J and Figure 5 H-J). An unpaired Student's t-test was employed to assess the effects of PNN degradation with ChABC on exploration in the open field (Figure S1 D-F), learning index (Figure 4 D & I), behavioral outcomes in the probe trial (Figure 4 E, F, J, K), cellular densities in the OFC (Figure 5), and synaptic densities in the OFC (Figure 6). P-values of ≤ 0.05 (two-tailed for Student's t-tests) or those adjusted for multiple comparisons using Tukey's HSD were considered statistically significant.

Results

Postnatal Enrichment Corrects Deficits in Reversal Learning in Adult LB Mice

We have previously shown that adolescent LB mice exhibit hyperactivity and significant cortical thinning, indicating that LB is a mouse model for early deprivation[21]. Given that childhood deprivation leads to substantial deficits in cognitive flexibility that are challenging to reverse through later adoption[2, 4, 5], we investigated the long-term effects of LB and LB combined with postnatal enrichment on reversal learning in the Barnes maze. Specifically, we established three rearing conditions: mice raised under control conditions (CTL), mice subjected to LB, and mice exposed to LB while also provided with toys in their home cage from P14 until P25, a condition we abbreviated as LBT (Figure 1 A-C). This 12-day period, roughly equivalent to ages 1 to 10 years in humans[28-31], was selected because it marks the time when mouse pups begin to actively explore their environment. Furthermore, several developmental processes, such as perineuronal net (PNN) formation, myelination, and synaptic pruning, which are essential for adult cognition and neuroplasticity, mature during this period in a manner that is highly sensitive to both deprivation and enrichment[21, 32-35].

Mice were weaned at P26 and tested in adulthood (P90-120) using the open field test on day 0. This was followed by four days of training in the Barnes maze (acquisition phase, days 1-

4) and an acquisition probe trial on day 5. Subsequently, mice underwent reversal learning from days 6 to 9, culminating in a reversal learning probe trial on day 10. Upon completion of the

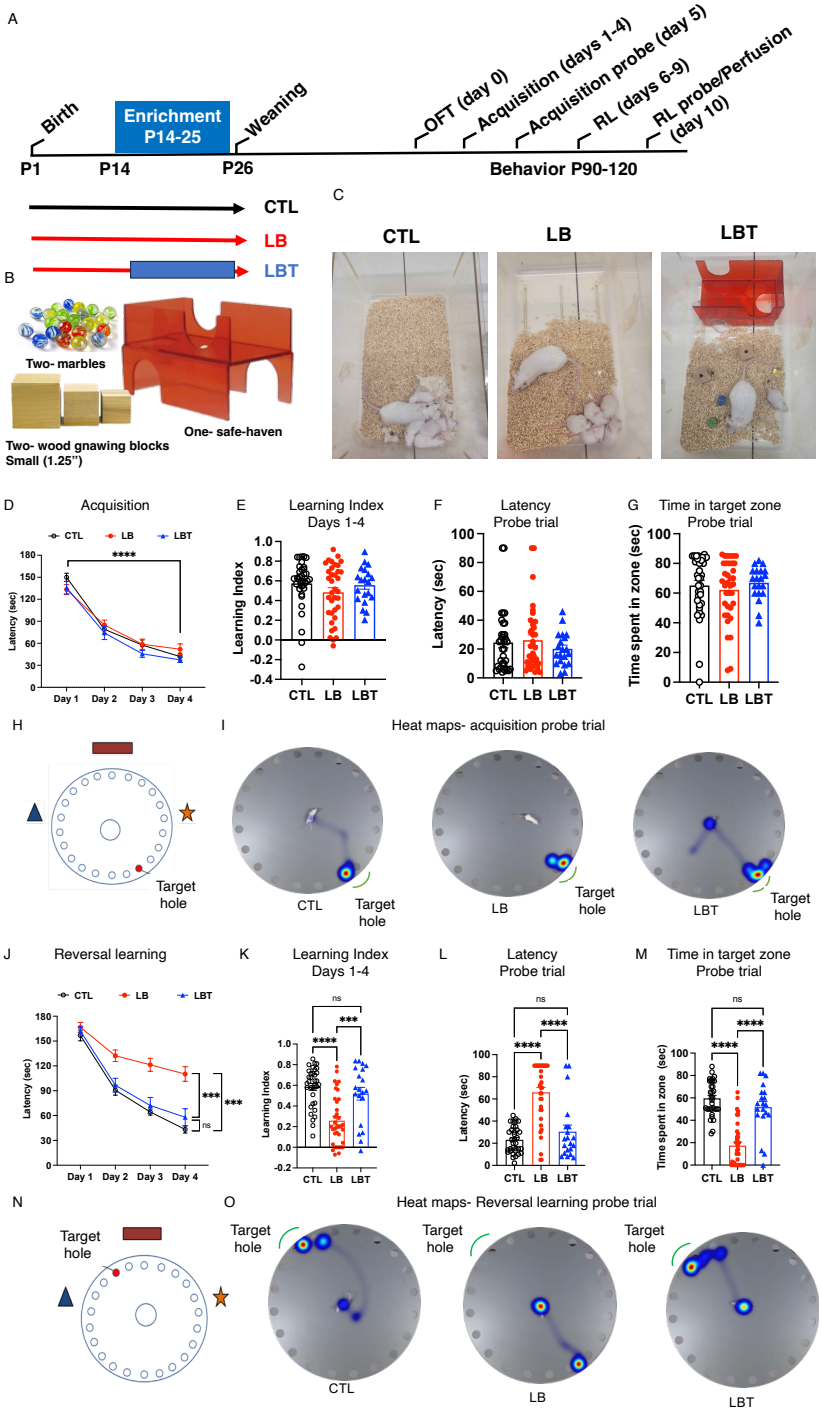

Figure 1. Early Enrichment Corrects Deficits in Reversal Learning Observed in Adult LB Mice. A. Experimental timeline. Acquisition D-I. Reversal learning (RL) J-O. **B.** Toys and objects used for postnatal enrichment. **C**. images of CTL, LB and LBT cages at P15. **D**. Acquisition (latency) days 1-4. rmANOVA, days: $F(2.4, 204.4)= 214$, $P< 0.001$, rearing: $F(2,84)= 0.45$, $P= 0.81$, sex: $F(1,84)= 0.52$, $P= 0.47$, interaction: $F(2,84)= 0.17$, $P= 0.84$. **E**. Acquisition (Learning

Index) days 1-4. ANOVA, rearing F (2, 84) = 1.50, P=0.23, sex F (1, 84) = 9.55, P= 0.0027, interaction: F (2, 84) = 0.14, P=0.86. **F**. Acquisition (probe trial) latency to escape. ANOVA, rearing F (2, 84) = 0.62, P= 0.53, sex: F (1, 84) = 8.92, P= 0.0037, interaction: F (2, 84) = 0.008, P= 0.99.**G**. Acquisition (probe trial) time in target zone. ANOVA, rearing F (2, 84) = 0.46, P= 0.62, sex: F (1, 84) = 2.91, P= 0.092, interaction: F (2, 84) = 0.34, P= 0.71. **H**. Schematic illustration of maze during acquisition phase. **I**. Representative heat maps of search strategy during acquisition probe trial. **J**. Reversal learning (latency) days 1-4. rmANOVA, days: F(2.35, 195.17)= 164.21, P< 0.001, rearing: F(2,83)= 20.62, P< 0.001, sex: F(1,83)= 0.27, P= 0.60, interaction: F(2,83)= 0.12, P= 088. Post-hoc. CTL vs. LB: P< 0.001, LBT vs. LB: P< 0.001, CTL vs. LBT: P= 0.58. **K**. Reversal learning (Learning Index) days 1-4. ANOVA, rearing F (2, 84) = 18.40, P< 0.000, sex: F (1, 84) = 0.67, P= 0.41, interaction: F (2, 84) = 0.21, P= 0.81. Post-hoc. CTL vs. LB: P <0.0001, LBT vs. LB: P= 0.0004, CTL vs. LBT: P= 0.69. **L**. Reversal learning (probe trial) latency to escape. ANOVA, rearing F (2, 84) = 35.86, P< 0.0001, sex: F (1, 84) = 1.75, P= 0.18, interaction: F (2, 84) = 0.95, P= 0.39. Post-hoc. CTL vs. LB: P <0.0001, LBT vs. LB: P <0.0001, CTL vs. LBT: P= 0.44. **M**. Reversal learning (probe trial) time in target zone. Rearing F (2, 84) = 50.20 P<0.0001, sex: F (1, 84) = 1.047 P=0.30, interaction F (2, 84) = 1.536 P=0.22. Post-hoc Sidak. CTL-LB P <0.0001, LBT-LB P <0.0001, CTL-LBT P= 0.2607. **N**. Schematic illustration of maze during reversal learning. **O**. Representative heat maps of search strategy during reversal learning probe trial. CTL males n=18, CTL females n= 18, LB males n= 18, LB females n=18, LBT males n=10, LBT females n=10. From 7-9 different litters per group.

reversal learning probe trial, mice were perfused to evaluate the effects of rearing conditions on c-fos activation in the OFC (Figure 1A). No main effects of rearing, sex, or their interaction were observed regarding the time spent in the center of the open field (Figure S1A). However, a significant interaction between rearing and sex was noted for distance traveled and velocity, attributed to the reduced velocity and overall distance traveled by LBT females compared to LB and CTL females (Figure S1 B-C). No significant differences in total distance traveled or average velocity were found among males (Figure S1 B-C). All groups exhibited a significant reduction in the latency to escape during the acquisition phase (rmANOVA, F(2.4, 204.4)= 214, P< 0.001) with no significant effects observed for rearing, sex, or the interaction between rearing and sex (Figure 1D and Figure S2 A-D for male and female data). Similarly, there were no significant effects of rearing, sex, or their interaction on the acquisition learning index. Additionally, no significant effects of rearing, sex, or interaction were found for the latency to escape and the time spent in the correct target during the probe trial (Figure 1 F-I). Collectively, these findings suggest that adult LB and LBT mice exhibit normal hippocampal-dependent memory.

In contrast, a significant effect of rearing was observed in reversal learning (F(2, 83) = 20.62, P< 0.001), with no significant effect of sex or interaction (Figure 1J). Post-hoc analysis revealed significant deficits in LB mice compared to CTL and LBT mice, with no differences between CTL and LBT mice (Figure 1J and Figure S2 E-H for separate male and female data). A similar pattern was noted for the reversal learning index, with LB mice exhibiting significant

362 impairments compared to both CTL and LBT mice, while LBT mice performed at a level
363 comparable to CTL mice (Figure 1K). During the reversal learning probe trial, LB mice took
364 longer to locate the escape hole (Figure 1L) and spent less time in the target quadrant
365 compared to CTL and LBT mice (Figure 1 M-O). LB mice predominantly searched around the
366 old escape hole, indicating a failure to adopt a new search strategy (Figure 1 I & O). These
367 findings reveal significant cognitive deficits in reversal learning in adult LB mice, which are fully
368 reversed by 12 days of enrichment during the second and third weeks of life.
369
370 **Enrichment Normalizes PNN Formation and c-fos activation in the OFC of Adult LB Mice**
371 At the completion of the reversal learning, mice were perfused to assess PNN formation
372 and c-fos activation in the OFC. We focused on the OFC because it is essential for reversal
373 learning[18, 36], and its development is compromised in individuals who have experienced
374 childhood deprivation[4, 13-17], with a significant correlation to the duration of that deprivation[2, 4].
375 PNNs are extracellular structures that primarily form around fast-spiking parvalbumin (PV) cells,
376 facilitating activity-dependent plasticity and various forms of learning[35, 37]. PNN formation begins
377 at P14 and peaks at P40 in the mouse OFC[34]. This developmental process is highly sensitive to
378 both deprivation and enrichment[35, 37, 38], making it a particularly compelling candidate for
379 mediating the mitigating effects observed in LBT. Indeed, the total number of PNN+ cells in the
380 OFC was significantly reduced in LB male and female mice compared to CTL and LBT groups,
381 with LBT mice exhibiting similar levels of PNN+ cells compared to CTL mice (Figure 2 A-B and
382 Figure S3A). Since PNNs predominantly form around PV+ cells—a process that appears to
383 protect these cells from oxidative stress[35, 37]—we also examined the effects of rearing, sex, and
384 their interaction on the density of PV+ cells in the OFC. A significant effect of rearing was
385 observed, but there were no significant effects of sex or interaction. Post-hoc analysis revealed
386 a significant reduction in the number of PV+ cells in LB mice compared to CTL and LBT groups,
387 with no significant differences between CTL and LBT (Figure 2 A & C and Figure S3B). The
388 density of c-fos positive cells in the OFC was significantly lower in LB compared to CTL and
389 LBT, with no significant differences between CTL and LBT (Figure 2 A & C and Figure S3C.
390 Using artificial intelligence and machine learning, we quantified the number of PNN+PV+,
391 PNN+PV-, and PNN-PV+ cells in the OFC (see Methods section and Figure 2A). Consistent
392 with previous studies[35, 37], the majority of PNN+ cells were PV+ (compare Figure 2 E to F & G),
393 and it was this population of PNN+PV+ cells that was significantly affected by LB and LBT
394 (Figure 2E). No significant effects of rearing, sex, or interaction were found for PNN+PV- (Figure
395 2F) and PNN-PV+ cells (Figure 2G). Significant correlations were identified between the number

of PNN+PV+ cells and performance in the probe trial of the reversal learning (Figure 2H), as well as c-fos activation in the OFC (Figure 2I). Furthermore, c-fos activation in the OFC was strongly correlated with performance in the probe trial of the reversal learning (Figure 2J). In summary, postnatal enrichment increases the density of PNN+PV+ cells in the OFC of adult LB mice to levels comparable to those observed in CTL mice, changes that may facilitate normal OFC activation and reversal learning in adulthood.

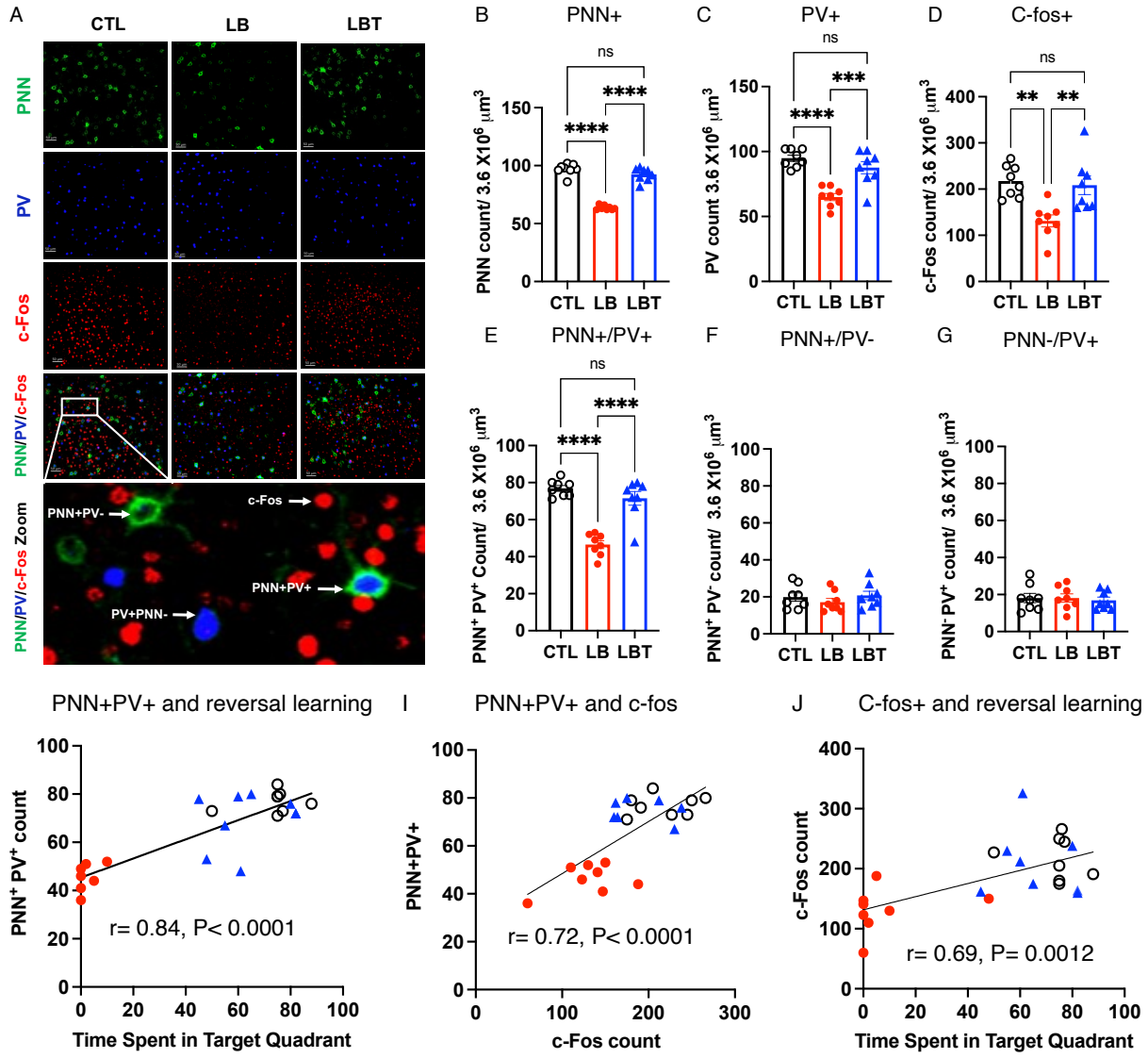

Figure 2. Postnatal Enrichment Mitigates Deficits in PNN Formation and Neuronal activation in the OFC of LB Mice A. Representative confocal images of PNN+, PV+, and c-fos+ cells in the OFC. Higher magnification image at the bottom depicts examples of PNN+PV+, PNN-PV+, PNN+PV-, and c-fos+ cells in the OFC. **B**. PNN+ cell density. ANOVA, rearing: F (2,18) = 135.3, P< 0.0001, sex: F (1,18) = 0.034, P=0.85, interaction: F (2,18) = 1.83, P= 0.19. Post-hoc, CTL vs. LB: P< 0.0001, LBT vs. LB: P< 0.0001, CTL vs. LBT: P= 0.17. **C**. PV+ cell density. ANOVA, rearing: F (2,18) = 18.55, P< 0.0001, sex: F (1,18) = 0.10, P= 0.75, interaction: F (2,18) = 0.39, P= 0.67. Post-hoc, CTL vs. LB: P< 0.0001, LBT vs. LB: P= 0.0009, CTL vs.

LBT: P= 0.35. **D**. c-fos+ cell density. ANOVA, rearing: F (2,18) = 10.54, P= 0.0009, sex: F (1,18) = 5.65, P= 0.029, interaction: F (2,18) = 0.074, P= 0.93. Post-hoc, CTL vs. LB: P= 0.0017, LBT vs. LB: P= 0.0045, CTL vs. LBT: P= 0.96. **E**. PNN+PV+ cell density. ANOVA, rearing: F (2,18) = 36.65, P< 0.0001, sex: F (1,18) = 0.61, P= 0.44, interaction: F (2,18) = 0.67, P= 0.52. Post-hoc, CTL vs. LB: P< 0.0001, LBT vs. LB: P< 0.0001, CTL vs. LBT: P= 0.35. **F**. PNN+PV- cell density. ANOVA, rearing: F (2,18) = 0.79, P= 0.46, sex: F (1,18) = 0.56, P= 0.46, interaction: F (2,18) = 2.01, P= 0.16. **G**. PNN-PV+ cell density. ANOVA, rearing: F (2,18) = 0.12, P= 0.88, sex: F (1,18) = 2.05, P= 0.17, interaction: F (2,18) = 1.89, P= 0.18. Pearson correlation between PNN+PV+ cell density and time spent in target quadrant (**H**), PNN+PV+ and c-fos+ cells (**I**), and c-fos+ cells and time spent in target quadrant (**J**). CTL n=8, LB n= 8, LBT n=8, half are females, from 5-6 different litters per group.

LB Increases the Ratio of Excitatory to Inhibitory Synapses in the OFC, an Effect That Was Reversed with Enrichment

PNN+PV+ cells enhance GABAergic tone and alter the excitatory-inhibitory (E-I) balance[37], prompting us to investigate the effects of rearing on the densities of GABAergic and glutamatergic synapses in the OFC. To achieve this, we first characterized the effects of rearing, sex, and their interaction on the densities of the presynaptic GABAergic marker (VGAT, Figure 3 A & B), the postsynaptic GABAergic marker (GEPHYRIN, Figure 3 A & C), and the density of putative GABAergic synapses, defined as sites where the two markers were in close proximity (< 250 nm, Figure 3 A & D). No significant effects of rearing, sex, or their interaction were observed for the total densities of VGAT (Figure 3B) or GEPHYRIN (Figure 3C). However, the density of putative GABAergic synapses was significantly reduced in the LB group compared to the CTL and LBT groups, with no differences observed between the CTL and LBT groups (Figure 3D). Additionally, there was a significant effect of sex, attributed to a slight reduction in the density of GABAergic synapses in females (Figure 3D).

A similar approach was employed to evaluate the effects of rearing conditions and sex on the density of the presynaptic glutamatergic marker VGlut2 (Figure 3 E & F), the postsynaptic marker PSD95 (Figure 3 E & G), and putative glutamatergic synapses (Figure 3 E & H). For VGlut2, we found a significant effect of both rearing and sex, but no significant interaction. Post-hoc analysis revealed a significant reduction in VGlut2 density in LBT compared to the LB group, with no significant differences between the CTL and the LB or LBT groups (Figure 3F). No significant effects of rearing, sex, or interaction were detected for the density of PSD95 puncta (Figure 3G). Significant effects of rearing and sex, but no significant interaction, were identified for the density of putative glutamatergic synapses in the OFC. Post-hoc analysis indicated that the rearing effect was attributed to an increase in glutamatergic synapses in LB compared to CTL and LBT with no significant difference between CTL and LBT (Figure 3H). The ratio of excitatory to inhibitory synapses in the OFC was approximately two-

fold higher in the LB group compared to the CTL and LBT groups in both males and females, with no differences observed between the CTL and LBT mice (Figure S4A). These findings align with previous research indicating that PNN+PV+ cells reduce E-I balance[37] and suggest that enrichment normalizes the elevated E-I ratio observed in the OFC of LB mice.

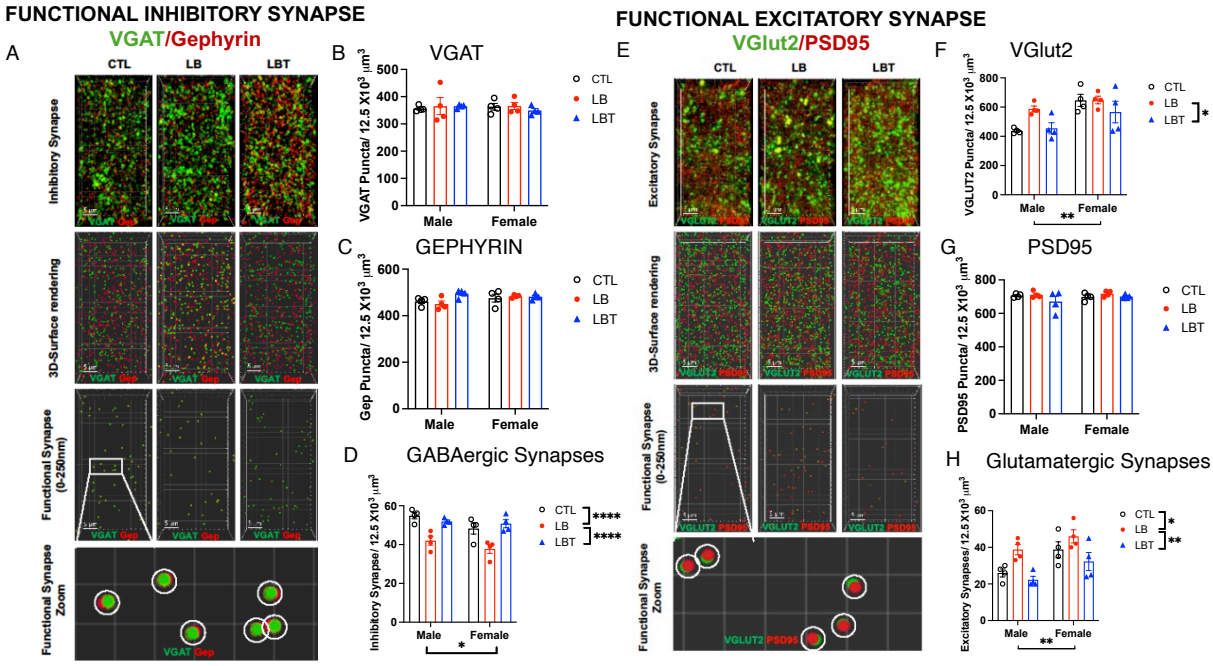

Figure 3. Effects of LB and LBT on GABAergic and glutamatergic synapse densities in the OFC. A. Confocal images and Imaris models of VGAT and GEPHYRIN staining in the OFC. **B**. VGAT puncta density. ANOVA, rearing: F (2,18) = 0.16, P= 0.85, sex: F (1,18) = 0.049, P= 0.83, interaction: F (2,18) = 0.29, P= 0.75. **C**. GEPHYRIN puncta density. ANOVA, rearing F(2,18) = 2.63, P=0.099, sex: F (1,18) = 1.80, P= 0.19, interaction: F (2,18) = 2.53, P= 0.11. **D**. GABAergic synapse density. ANOVA, rearing: F (2,18) = 20.43, P< 0.0001, sex: F (1,18) = 5.55, P= 0.03, interaction: F (2,18) = 0.85, P= 0.44. Post-hoc, CTL vs. LB: P< 0.0001, LBT vs. LB: P< 0.0001, CTL vs. LBT: P= 0.99. **E**. Confocal images and Imaris models of VGlut2 and PSD95 staining in the OFC. **F**. VGlut2 puncta density. ANOVA, rearing: F (2,18) = 3.72, P= 0.044, sex F (1,18) = 14.88, P=0.0012, interaction: F (2,18) = 1.75, P= 0.20. Post-hoc, CTL vs. LB: P= 0.20, LBT vs. LB: P= 0.048, CTL vs. LBT: P= 0.84. **G**. PSD95 puncta density. ANOVA, rearing: F (2,18) = 1.75, P=0.20, sex: F (1,18) = 0.65, P= 0.43, interaction: F (2,18) = 0.79, P= 0.46. **H**. Glutamatergic synapse density. ANOVA, rearing F (2,18) = 9.92, P= 0.0012, sex: F (1, 18) = 12.57, P= 0.0023, interaction: F (2,18) = 0.32, P= 0.73. Post-hoc, CTL vs. LB: P= 0.025, LBT vs. LB: P= 0.001, CTL vs. LBT: P= 0.32. CTL n=8, LB n= 8, LBT n=8, half are females, from 5-6 different litters per group.

ChABC Degradation of PNN in the OFC Impairs Reversal Learning

Although PNN+PV+ cells have been shown to facilitate various forms of learning[35, 37, 38], it remains unclear whether PNN+PV+ cells in the OFC are essential for reversal learning. To investigate this question, we first developed a protocol to reduce the number of PNN+PV+ cells in the OFC to levels observed in LB mice. As an initial step, we injected ChABC into the right

OFC and a vehicle solution into the left OFC of adult CTL male mice (n=3). Seven days later, the mice were perfused to compare the densities of PNN+, PV+, and PNN+PV+ cells in the OFC (Figure S5). As expected, the densities of PNN+, PV+, and PNN+PV+ cells in the ChABC-injected OFC were significantly lower compared to those in the vehicle-injected side (Figure S5). Interestingly, ChABC treatment did not impact the density of PNN+PV- suggesting that it is more effectively targeting PNN+PV+ cells (Figure S5 and figure 5). Next, we administered ChABC or vehicle bilaterally into the OFC of adult CTL males (n=14-15 mice per group). After a 7-day recovery period, the mice were tested for exploratory behavior in the open field test, as well as for acquisition and reversal learning using the same procedures applied to LB and LBT groups (Figure 4A). ChABC treatment did not impact exploratory behavior in the open field test (Figure S1 D-F) and had no effect on acquisition learning or performance in the probe trial (Figure 4 C-G). In contrast, PNN degradation impaired reversal learning, with vehicle-treated mice showing a significant reduction in the latency to escape, while ChABC-treated mice showed no significant improvement over time (Figure 4H). The reversal learning index was lower ChABC-treated mice, but this reduction was not significant (Figure 4I). In the probe trial, the ChABC treatment significantly increased the latency to escape 4J) and the and reduced the time spent in the correct target (Figure K-L).

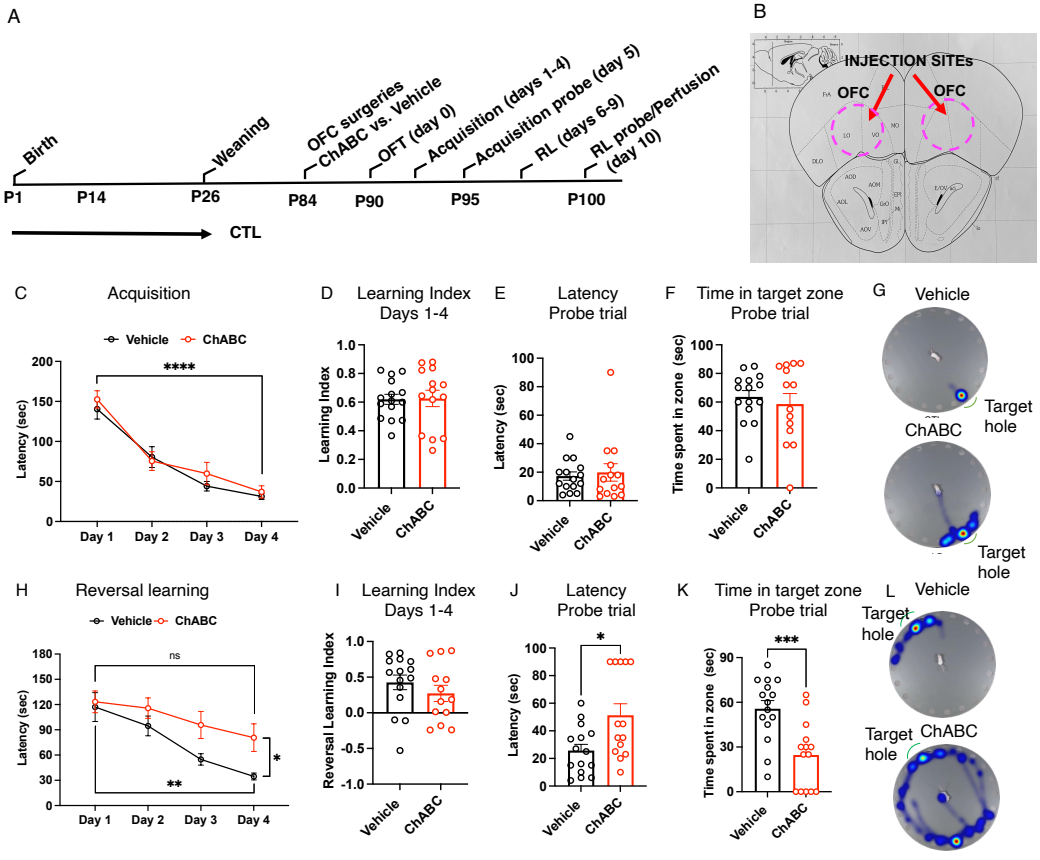

Figure 4. PNN Degradation in the OFC Impairs Reversal Learning. A. Experimental timeline. **B**. Schematics of OFC targeting. **C**. Acquisition (latency) days 1-4. Days of training: $F(2.296,61.98) = 78.09$, $P<0.0001$, treatment: $F(1,27) = 0.41$, $P= 0.53$, interaction: $F(3,81) = 0.67$, $P= 0.57$.**D**. Acquisition (Learning Index) days 1-4. Treatment: $t(27)= 0.092$, $P= 0.93$. **E**. Acquisition (probe trial) latency to escape. Treatment: $t(27)= 0.39$, $P= 0.69$. **F**. Acquisition (probe trial) time in target zone. Treatment: $t(27)=0.58$, $P= 0.56$. **G**. Heat maps of acquisition probe trial. **H**. Reversal learning (latency) days 1-4. Days of training: $F(2.172, 58.66) = 17.36$, $P<0.0001$, treatment: $F(1, 27) = 4.31$, $P= 0.048$, interaction: $F(3,81) = 1.84$, $P= 0.15$. **I**. Reversal learning (Learning Index) days 1-4. Treatment $t(26)= 1.01$, $P= 0.32$. **J**. Reversal learning (probe trial) latency to escape. Treatment: $t(27) = 2.74$, $P= 0.011$.**K**. Reversal learning (probe trial) time in target zone. Treatment $t(27) =3.824$, $P= 0.0007$. L. Heat maps acquisition probe trial. rmANOVA: C & H. Student-t-tests: D-F, I-K. Vehicle n= 15, ChABC n=14, all males.

ChABC Administration Reduces PNN+PV+ and c-fos Activation in the OFC

Ninety minutes after completing the probe trial, mice were perfused to evaluate the effects of ChABC treatment on PNN degradation, PV+ cell density, and c-fos activation in the OFC. ChABC treatment reduced the total number of PNN+ cells in the OFC by approximately 40% (Figure 5 A & B), bringing levels in line with those observed in adult LB mice (Figure 2D). Additionally, ChABC treatment decreased the number of PV+ cells in the OFC (Figure 5C), which is consistent with previous studies suggesting a protective role[35, 37]. PNN degradation also led to a reduction in the densities of c-fos+ cells (Figure 5D) and PNN+PV+ cells in the OFC. However, the densities of PNN+PV- (Figure 5F) and PNN-PV+ cells (Figure 5G) remained unaffected, indicating that ChABC preferentially targeted PNN+PV+ cells. In line with our findings in LB mice (Figure 2 H-J), there was a significant correlation between the number of PNN+PV+ cells, performance in the probe trial, and c-fos activation in the OFC (Figure 5 H-J). These studies demonstrate that a high density of PNN+PV+ cells in the OFC is essential for normal c-fos activation and reversal learning.

ChABC Increases the Ratio between Excitatory and Inhibitory Synapses in the OFC

ChABC treatment did not affect the total densities of VGAT (Figure 6 A & B) and GEPHYRIN (Figure 6 A & C), but it did reduce the density of putative GABAergic synapses (Figure 6 A & D). PNN degradation had no significant impact on the densities of VGlut2 puncta (Figure 6 E & F), PSD95 puncta (Figure 6 E & G), or the putative glutamatergic synapses in the OFC (Figure 6 E & H). The ratio of excitatory to inhibitory synapses in the OFC increased in ChABC mice, reaching levels comparable to those observed in LB mice (Figure S4B). In summary, PNN degradation and exposure to LB resulted in similar synaptic changes in the OFC.

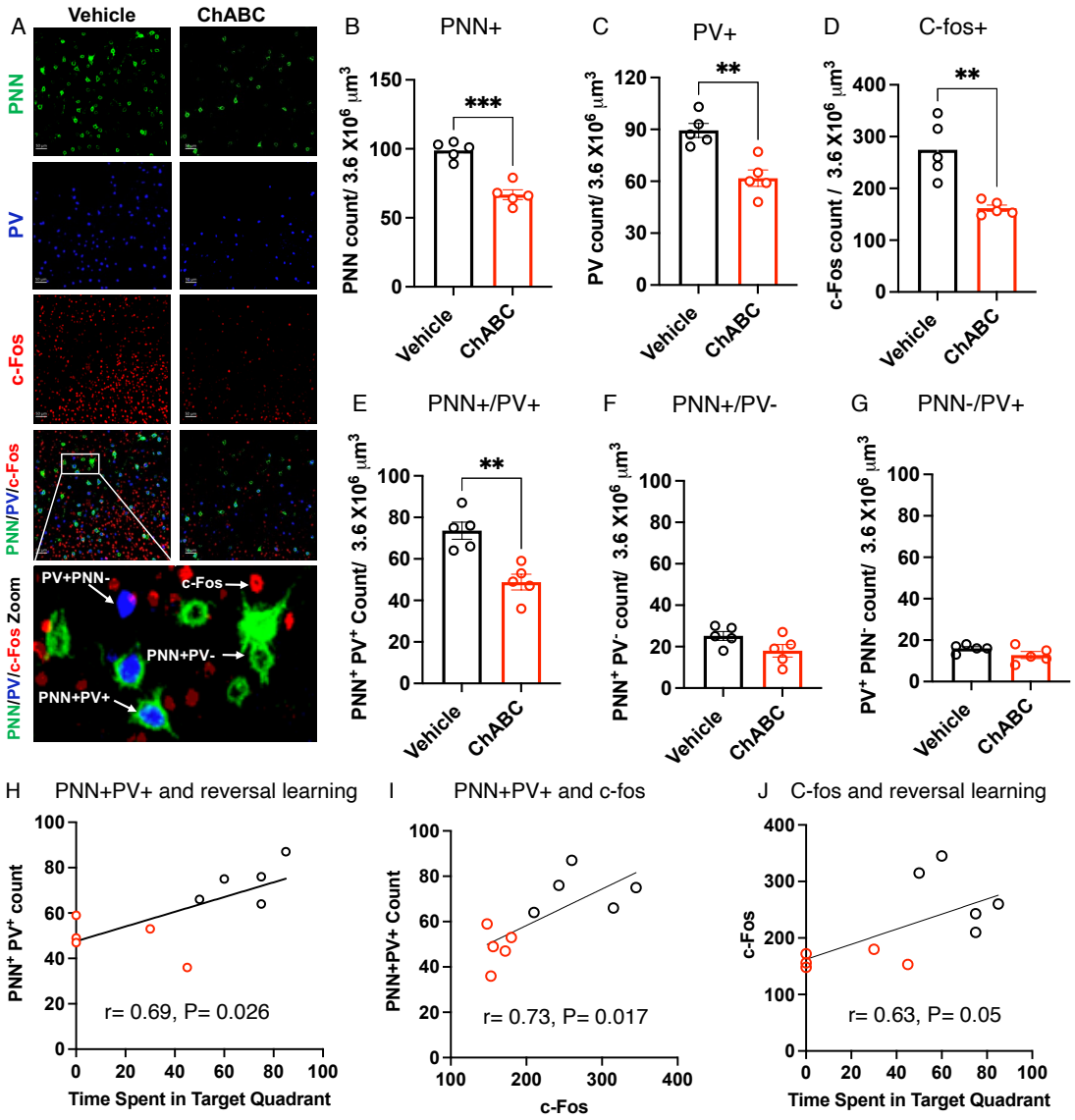

Figure 5. ChABC Treatment Targets PNN+PV+ cells and impairs Neuronal Activation in the OFC During Reversal Learning. A. Representative confocal images of PNN+, PV+, and c-fos+ cells in the OFC. Higher magnification image at the bottom depicts examples of PNN+PV+, PNN-PV+, PNN+PV-, and c-fos+ cells in the OFC. **B**. PNN+ cell density, t(8)= 6.99, P= 0.0001. **C**. PV+ cell density, t(8)= 4.47, P= 0.0021. **D**. c-fos cell density, t(8)=4.475, P= 0.0021. **E**. PNN+PV+ cell density, t(8)= 4.433, P= 0.0022. **F**. PNN+PV- cell density, t(8)=1.93, P= 0.090. **G**. PNN-PV+, t(8)=1.677, P= 0.132. Pearson correlation between PNN+PV+ cell density and time spent in target quadrant (**H**), PNN+PV+ and c-fos+ cells (**I**), and c-fos+ cells and time spent in target quadrant (**J**). Student-t-tests: B-G. Vehicle n= 5, ChABC n= 5, all males.

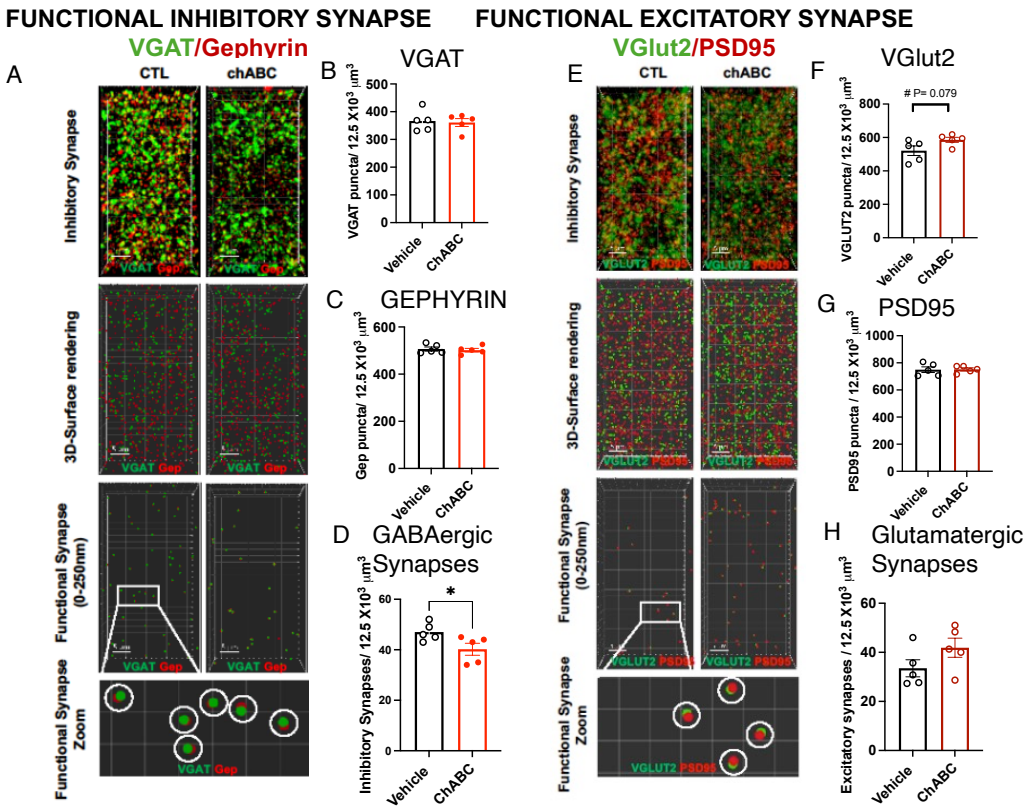

Fig 6. PNN Degradation Reduces GABAergic Synapse Density in the OFC. A. Confocal images and Imaris models of VGAT and GEPHYRIN staining in the OFC. **B**. VGAT puncta density, t (8)= 0.25, P= 0.81. **C**. GEPHYRIN puncta density, t(8)=0.42, P= 0.68. **D**. GABAergic synapse density, t(8)= 2.398, P= 0.043. **E**. Confocal images and Imaris models of VGlut2 and PSD95 staining in the OFC. **F**. VGlut2 puncta density, t(8)= 2.016, P= 0.079. **G**. PSD95 puncta density, t(8)= 0.099, P= 0.92. **H**. Glutamatergic synapse density t(8)= 1.61, P= 0.15. Student-t-tests: B-G. Vehicle n= 5, ChABC n= 5, all males.

Discussion

Childhood neglect and deprivation are associated with abnormal development and function of the OFC[4, 13-17]. The duration of deprivation correlates with the extent of volumetric reduction in the OFC and is not reversed through adoption[4]. Given that the OFC plays a central role in mediating cognitive flexibility and adaptability[18], it is reasonable to speculate that abnormalities in OFC function contribute significantly to the long-term and complex psychopathology associated with neglect and deprivation. Despite being the most prevalent form of ELA, little is currently understood about the mechanisms responsible for these developmental changes, and no animal models have yet successfully replicated the key structural and behavioral features associated with childhood deprivation and neglect. To investigate these questions, we have recently demonstrated that adolescent mice raised in impoverished conditions, characterized by limited bedding and no nesting (LB), exhibit

hyperactivity and significant cortical thinning, suggesting that LB serves as a valid mouse model of neglect and deprivation[21]. In this study, we further substantiate this assertion by showing that LB leads to severe long-term deficits in reversal learning, which can be fully mitigated by a brief enrichment protocol administered from P14 until P25. This is the first study to demonstrate that postnatal enrichment can reverse cognitive deficits associated with LB, one of the most commonly used rodent models of ELA[39]. Enrichment corrects deficits in neuronal activation during reversal learning probe trial and normalizes the number of PNN+PV+ cells in the OFC. The degradation of PNN surrounding PV+ cells in the OFC to levels observed in LB mice mimics the cognitive, c-fos activation, and synaptic deficits seen in the OFC of LB mice. Collectively, these findings suggest that early deprivation and enrichment regulate cognitive flexibility by altering the PNN+PV+ levels in the OFC.

To the best of our knowledge, only one additional study has examined the impact of limited bedding and nesting on reversal learning in adult mice[36]. Goodwill and colleagues utilized a shorter paradigm of limited bedding and nesting that extended from P4 to P11 in C57 mice. They reported deficits in rule-reversal learning in adult female mice, which were not observed in their male littermates. These deficits were associated with a reduced number of PV+ cells in the OFC of females, but not males. Furthermore, optogenetic inhibition of PV+ cells in the OFC replicated the rule-reversal learning deficits seen in females[36]. These findings align with our own, as they link LB induced deficits in reversal learning to abnormal development and function of PV+ cells in the OFC. Our data extend these findings by demonstrating that abnormal PNN formation around PV+ cells is responsible for the deficits in reversal learning. We also show that LB increases GABAergic synapse density, increases E-I balance, and impairs c-fos activation in the OFC. Importantly, all these changes were reversed by postnatal enrichment and were mimicked by PNN degradation in the OFC. However, it remains unclear why only females were affected in the Goodwill et al. (2018) study, while our study found impacts in both males and females. We suspect that these divergent outcomes may be attributed to the shorter exposure to LB used by Goodwill and colleagues (P4-11 vs. P0-25), differences in the testing paradigms (e.g., attentional set shifting vs. Barnes maze), or variations in mouse strains (C57BL/6 versus Balb/cByj).

Three additional studies have investigated the impact of various versions of the LB paradigm on the density of PV+PNN+ cells[35, 40, 41]. Santiago et al. (2018) reported that juvenile rats (P22-23) exposed to limited bedding and nesting from P8 to P12 exhibited reduced PNN staining around PV+ cells in the anterior basolateral amygdala (BLA)[40]. In contrast, exposure to limited bedding from P1-10 increased the density of PV+PNN+ cells in the BLA of P28 males,

but not in female rats[41]. Exposure to LB from P2-9 in C57 mice resulted in an increased density of PNN+ cells in the medial prefrontal cortex of adult (P70) male and female mice[35]. These discrepancies are likely attributable to variations in the duration and developmental timing of LB exposure, the species studied, and the specific brain regions examined. The duration and timing of LB exposure appear to be critical factors, as PNN development typically begins around P14[34] and, as demonstrated in this study and by others, is highly sensitive to environmental enrichment and manipulations during the subsequent two weeks[35, 37]. Notably, Santiago and colleagues reported that exposure to LB from P8 to P12 led to a significant decrease in the density of PV+PNN+ cells in the BLA at P15, but not at P18[40]. We hypothesize that extending their LB exposure to P18 would result in a sustained reduction in the density of PV+PNN+ cells at this age. In other words, prolonging LB exposure to P25, as conducted in this study, may be necessary to induce a robust and sustained reduction in PNN formation. One human study examining the effects of early life adversity on PNN formation found a significant increase in the density of PV+PNN+ cells in the ventromedial prefrontal cortex[42]. However, this investigation focused exclusively on individuals who experienced severe physical and sexual abuse early in life[42], and its findings may not be applicable to individuals who faced childhood neglect and deprivation.

Several observations highlight the appeal of PNN development as a cellular target for mediating long-term cognitive deficits associated with neglect and deprivation. First, PNN development is highly sensitive to both environmental deprivation and enrichment[35, 37, 38, 43]. Second, it is essential to limit earlier forms of plasticity and to stabilize synaptic organization[35, 37, 43]. Third, it supports adult plasticity and learning by altering E-I balance and gamma oscillations[35, 37, 38]. In essence, PNN maturation facilitates the transition from an earlier form of postnatal plasticity, which relies on synaptic reorganization, to a different form of adult plasticity that is driven by GABAergic modulation of adult circuits.

In summary, our study implicates the formation of PNNs in the OFC as a crucial step in the ability of early enrichment to correct deficits in cognitive flexibility in a mouse model of early neglect and deprivation. These findings raise several follow-up questions that require further investigation. For instance, additional research is needed to clarify the mechanisms by which LB and LBT alter PNN formation in the OFC. One possibility is that deprivation and enrichment influence PNN formation by regulating the expression of the transcription factor OTX2[43] or the expression of key components of PNN synthesized by glial cells[35, 37]. Another possibility is that deprivation and enrichment affect PNN degradation through enzymes such as metalloproteinases or via direct microglial-mediated phagocytic activity[35, 44]. Additional studies

are also necessary to clarify how PNN+PV+ cells enhance c-fos activation in the OFC and how the activation of these putative glutamatergic neurons facilitates performance in reversal learning. Finally, it would be interesting to know whether administering a similar enrichment protocol in adult LB mice would be as effective in enhancing PNN formation in the OFC and correcting deficits in reversal learning. Clarifying this latter question will likely have important clinical implications regarding the optimal timing for interventions.

Acknowledgements

We would like to thank our funding sources: NIMH R01MH119164, NIMH R01MH118332, NIMH R01MH136490, and the Clinical Neuroscience Division of the VA National Center for PTSD.

Conflict of Interest

The authors declare no conflict of interest.

References

1. U.S. Department of Health & Human Services AoC, Youth and Families, Children's Bureau. Child Maltreatment 2022. https://www.acf.hhs.gov/cb/data-research/child-maltreatment., 2024.

2. McLaughlin KA, Sheridan MA, Nelson CA. Neglect as a Violation of Species-Expectant Experience: Neurodevelopmental Consequences. *Biol Psychiatry* 2017; **82**(7)**:** 462-471.

3. De Bellis MD. The psychobiology of neglect. *Child Maltreat* 2005; **10**(2)**:** 150-172.

4. Mackes NK *et al.* Early childhood deprivation is associated with alterations in adult brain structure despite subsequent environmental enrichment. *Proc Natl Acad Sci U S A* 2020; **117**(1)**:** 641-649.

5. Spratt EG *et al.* The Effects of Early Neglect on Cognitive, Language, and Behavioral Functioning in Childhood. *Psychology (Irvine)* 2012; **3**(2)**:** 175-182.

6. Martin AJ, Nejad H, Colmar S, Liem GAD. Adaptability: Conceptual and Empirical Perspectives on Responses to Change, Novelty and Uncertainty. *Australian Journal of Guidance and Counselling* 2012; **22**(1)**:** 58-81.

7. Franken K *et al.* Introduction of the generic sense of ability to adapt scale and validation in a sample of outpatient adults with mental health problems. *Frontiers in psychology* 2023; **14:** 985408.

8. Zhou M, Lin W. Adaptability and Life Satisfaction: The Moderating Role of Social Support. *Frontiers in psychology* 2016; **7:** 1134.

9. Feraco T, Sella E, Meneghetti C, Cona G. Adapt, Explore, or Keep Going? The Role of Adaptability, Curiosity, and Perseverance in a Network of Study-Related Factors and Scholastic Success. *J Intell* 2023; **11**(2).

10. Herruzo C, Raya Trenas A, Pino MJ, Herruzo J. Study of the Differential Consequences of Neglect and Poverty on Adaptive and Maladaptive Behavior in Children. *Int J Environ Res Public Health* 2020; **17**(3).

11. Wooten W, Laubaucher C, George GC, Heyn S, Herringa RJ. The impact of childhood maltreatment on adaptive emotion regulation strategies. *Child Abuse Negl* 2022; **125:** 105494.

12. Manly JT, Lynch M, Oshri A, Herzog M, Wortel SN. The impact of neglect on initial adaptation to school. *Child Maltreat* 2013; **18**(3)**:** 155-170.

13. Bounoua N, Miglin R, Spielberg JM, Johnson CL, Sadeh N. Childhood trauma moderates morphometric associations between orbitofrontal cortex and amygdala: implications for pathological personality traits. *Psychol Med* 2022; **52**(13)**:** 2578-2587.

14. Hanson JL *et al.* Early stress is associated with alterations in the orbitofrontal cortex: a tensor-based morphometry investigation of brain structure and behavioral risk. *J Neurosci* 2010; **30**(22)**:** 7466-7472.

15. Holz NE *et al.* The long-term impact of early life poverty on orbitofrontal cortex volume in adulthood: results from a prospective study over 25 years. *Neuropsychopharmacology* 2015; **40**(4)**:** 996-1004.

16. Monninger M *et al.* The Long-Term Impact of Early Life Stress on Orbitofrontal Cortical Thickness. *Cereb Cortex* 2020; **30**(3)**:** 1307-1317.

17. Wang L *et al.* Childhood trauma and cognitive deficits in patients with schizophrenia: mediation by orbitofrontal cortex H-shaped sulci volume. *J Psychiatry Neurosci* 2022; **47**(3)**:** E209-E217.

18. Izquierdo A, Brigman JL, Radke AK, Rudebeck PH, Holmes A. The neural basis of reversal learning: An updated perspective. *Neuroscience* 2017; **345:** 12-26.

19. Sedlak AJ *et al.* Fourth National Incidence Study of Child Abuse and Neglect (NIS–4): Report to Congress. U.S. Department of Health and Human Services, Administration for Children and Families.: Washington, DC, 2010.

20. Lambert HK *et al.* Hippocampal Contribution to Context Encoding across Development Is Disrupted following Early-Life Adversity. *J Neurosci* 2017; **37**(7)**:** 1925-1934.

21. Islam R *et al.* Early Adversity Causes Sex-Specific Deficits in Perforant Pathway Connectivity and Contextual Memory in Adolescent Mice. *Biology of sex differences* 2024; **15**(article number 39).

22. van Praag H, Kempermann G, Gage FH. Neural consequences of environmental enrichment. *Nat Rev Neurosci* 2000; **1**(3)**:** 191-198.

23. Bredy TW, Zhang TY, Grant RJ, Diorio J, Meaney MJ. Peripubertal environmental enrichment reverses the effects of maternal care on hippocampal development and glutamate receptor subunit expression. *Eur J Neurosci* 2004; **20**(5)**:** 1355-1362.

24. Curley JP, Davidson S, Bateson P, Champagne FA. Social enrichment during postnatal development induces transgenerational effects on emotional and reproductive behavior in mice. *Frontiers in behavioral neuroscience* 2009; **3:** 25.

25. Goldstein EZ, Pertsovskaya V, Forbes TA, Dupree JL, Gallo V. Prolonged Environmental Enrichment Promotes Developmental Myelination. *Front Cell Dev Biol* 2021; **9:** 665409.

26. Ball NJ, Mercado E, 3rd, Orduna I. Enriched Environments as a Potential Treatment for Developmental Disorders: A Critical Assessment. *Frontiers in psychology* 2019; **10:** 466.

27. Ahmed S *et al.* Transient impairment in microglial function causes sex-specific deficits in synaptic maturity and hippocampal function in mice exposed to early adversity. *Brain, behavior, and immunity* 2024; **122:** 95-109.

28. Seress L. Comparative anatomy of the hippocampal dentate gyrus in adult and developing rodents, non-human primates and humans. *Prog Brain Res* 2007; **163:** 23-41.

29. Workman AD, Charvet CJ, Clancy B, Darlington RB, Finlay BL. Modeling transformations of neurodevelopmental sequences across mammalian species. *J Neurosci* 2013; **33**(17)**:** 7368-7383.

30. Zeiss CJ. Comparative Milestones in Rodent and Human Postnatal Central Nervous System Development. *Toxicol Pathol* 2021; **49**(8)**:** 1368-1373.

31. Abraham H *et al.* Myelination in the human hippocampal formation from midgestation to adulthood. *Int J Dev Neurosci* 2010; **28**(5)**:** 401-410.

32. Islam R, Kaffman A. White-matter repair as a novel therapeutic target for early adversity *Front neurosci* 2021.

33. Ahmed S, Polis B, Kaffman A. Microglia: The Drunken Gardeners of Early Adversity. *Biomolecules* 2024; **14**(8).

34. Bruckner G *et al.* Postnatal development of perineuronal nets in wild-type mice and in a mutant deficient in tenascin-R. *J Comp Neurol* 2000; **428**(4)**:** 616-629.

35. Belliveau C *et al.* Postmortem evidence of microglial involvement in the child abuse-associated increase of perineuronal nets in the ventromedial prefrontal cortex. *BioRxiv* 2024.

36. Goodwill HL *et al.* Early Life Stress Drives Sex-Selective Impairment in Reversal Learning by Affecting Parvalbumin Interneurons in Orbitofrontal Cortex of Mice. *Cell reports* 2018; **25**(9)**:** 2299-2307 e2294.

37. Tewari BP, Chaunsali L, Prim CE, Sontheimer H. A glial perspective on the extracellular matrix and perineuronal net remodeling in the central nervous system. *Frontiers in cellular neuroscience* 2022; **16:** 1022754.

38. Favuzzi E *et al.* Activity-Dependent Gating of Parvalbumin Interneuron Function by the Perineuronal Net Protein Brevican. *Neuron* 2017; **95**(3)**:** 639-655 e610.

39. Walker CD *et al.* Chronic early life stress induced by limited bedding and nesting (LBN) material in rodents: critical considerations of methodology, outcomes and translational potential. *Stress* 2017; **20**(5)**:** 421-448.

40. Santiago AN, Lim KY, Opendak M, Sullivan RM, Aoki C. Early life trauma increases threat response of peri-weaning rats, reduction of axo-somatic synapses formed by parvalbumin cells and perineuronal net in the basolateral nucleus of amygdala. *J Comp Neurol* 2018; **526**(16)**:** 2647-2664.

41. Guadagno A, Verlezza S, Long H, Wong TP, Walker CD. It Is All in the Right Amygdala: Increased Synaptic Plasticity and Perineuronal Nets in Male, But Not Female, Juvenile Rat Pups after Exposure to Early-Life Stress. *J Neurosci* 2020; **40**(43)**:** 8276-8291.

42. Tanti A *et al.* Child abuse associates with increased recruitment of perineuronal nets in the ventromedial prefrontal cortex: a possible implication of oligodendrocyte progenitor cells. *Mol Psychiatry* 2022; **27**(3)**:** 1552-1561.

43. Bernard C, Prochiantz A. Otx2-PNN Interaction to Regulate Cortical Plasticity. *Neural Plast* 2016; **2016:** 7931693.

44. Rahimian R, Belliveau C, Simard S, Turecki G, Mechawar N. Perineuronal Net Alterations Following Early-Life Stress: Are Microglia Pulling Some Strings? *Biomolecules* 2024; **14**(9).

Supplemental Information (Figures S1-5).

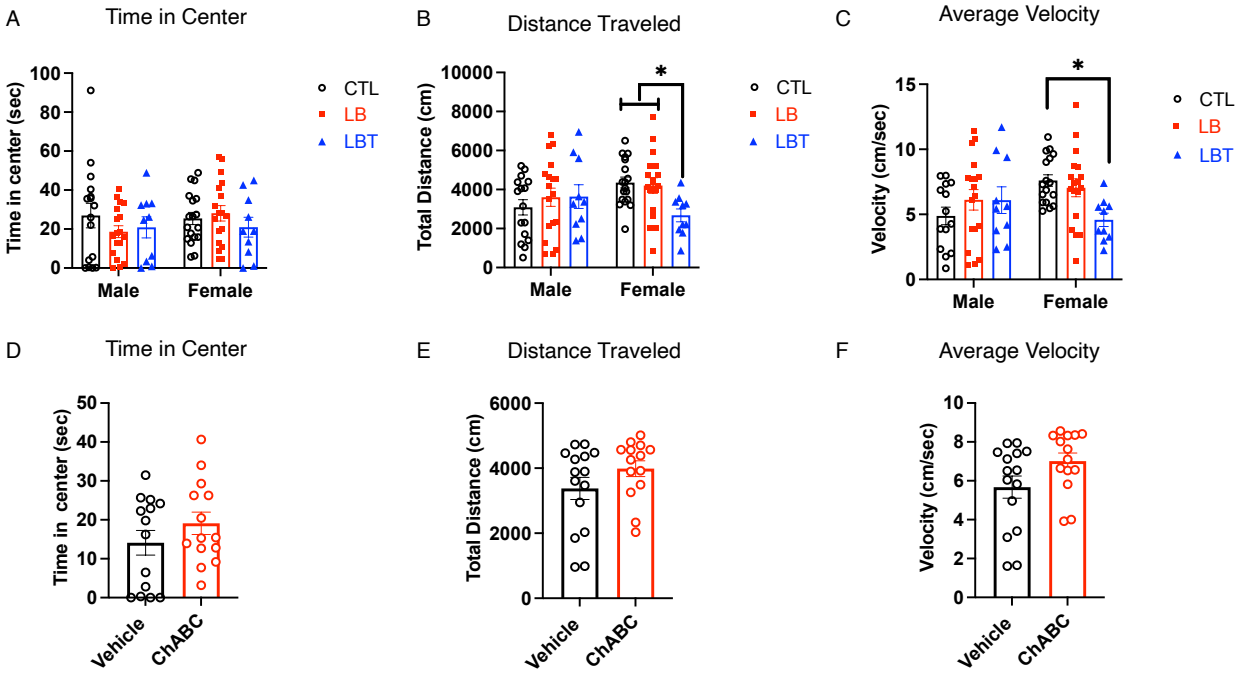

Fig S1. Exploratory Behavior in the Open Field. Effects of rearing conditions (A-C) and PNN degradation in the OFC (D-E). **A**. Time in the center, rearing: F (2, 84) = 0.61, P=0.54, sex: F (1, 84) = 0.50, P=0.48, interaction: F (2, 84) = 0.98, P= 0.38. **B**. Distance traveled, rearing: F (2, 84) = 1.39, P=0.25, sex: F (1, 84) = 0.73, P= 0.39, interaction: F (2, 84) = 3.00, P= 0.054. Post-hoc analysis males: CTL vs. LB: P= 0.62, CTL vs. LBT: P= 0.67, LB vs. LBT: P= 0.99. Post-hoc analysis females: CTL vs. LB: P= 0.96, CTL vs LBT: P= 0.027, LB vs. LBT: P= 0.049. **C**. Velocity, rearing: F (2, 81) = 1.38, P= 0.26, sex: F (1, 81) = 1.42, P= 0.23, interaction: F (2, 81) = 3.75. P=0.028. Post-hoc analysis males: CTL vs. LB: P= 0.41, CTL vs. LBT: P= 0.52, LB vs. LBT: P= 0.99. Post-hoc analysis females: CTL vs. LB: P= 0.81, CTL vs. LBT: P= 0.017, LB vs. LBT: P= 0.059. **D**. Time in center, t(26)= 1.17, P= 0.25. **E**. Distance traveled, t(27)= 1.43, P= 0.16. **F.** Velocity, t(27)= 1.88, P= 0.07. A-C, two-way ANOVA, CTL males n=18, CTL females n= 18, LB males n= 18, LB females n=18, LBT males n=10, LBT females n=10. From 7-9 different litters per group. D-F, student-t-tests, Vehicle n= 15, ChABC n=14, all males.

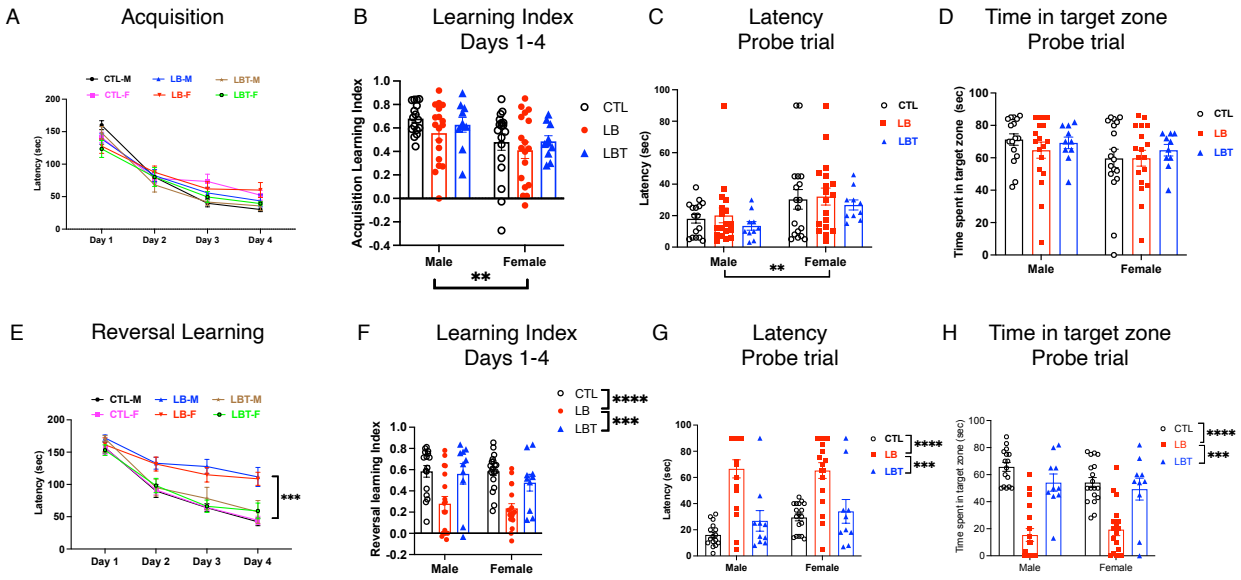

Fig S2. Effects of Rearing and Sex on Acquisition Phase (A-D) and Reversal Learning (E-H). This is the same data shown in Figure 1 except that outcomes in males and females are shown separately. **A**. Acquisition (latency) days 1-4. rmANOVA, days: $F(2.4, 204.4)= 214$, $P< 0.001$, rearing: $F(2,84)= 0.45$, $P= 0.81$, sex: $F(1,84)= 0.52$, $P= 0.47$, interaction: $F(2,84)= 0.17$, $P= 0.84$. **B**. Acquisition (Learning Index) days 1-4. ANOVA, rearing $F (2, 84) = 1.50$, $P=0.23$, sex $F (1, 84) = 9.55$, $P= 0.0027$, interaction: $F (2, 84) = 0.14$, $P=0.86$. **C**. Acquisition (probe trial) latency to escape. ANOVA, rearing $F (2, 84) = 0.62$, $P= 0.53$, sex: $F (1, 84) = 8.92$, $P= 0.0037$, interaction: $F (2, 84) = 0.008$, $P= 0.99$.**D**. Acquisition (probe trial) time in target zone. ANOVA, rearing $F (2, 84) = 0.46$, $P= 0.62$, sex: $F (1, 84) = 2.91$, $P= 0.092$, interaction: $F (2, 84) = 0.34$, $P= 0.71$. **E**. Reversal learning (latency) days 1-4. rmANOVA, days: $F(2.35, 195.17)= 164.21$, $P< 0.001$, rearing: $F(2,83)= 20.62$, $P< 0.001$, sex: $F(1,83)= 0.27$, $P= 0.60$, interaction: $F(2,83)= 0.12$, $P= 088$. Post-hoc. CTL vs. LB: $P< 0.001$, LBT vs. LB: $P< 0.001$, CTL vs. LBT: $P= 0.58$. **F**. Reversal learning (Learning Index) days 1-4. ANOVA, rearing $F (2, 84) = 18.40$, $P< 0.000$, sex: $F (1, 84) = 0.67$, $P= 0.41$, interaction: $F (2, 84) = 0.21$, $P= 0.81$. Post-hoc. CTL vs. LB: $P <0.0001$, LBT vs. LB: $P= 0.0004$, CTL vs. LBT: $P= 0.69$. **G**. Reversal learning (probe trial) latency to escape. ANOVA, rearing $F (2, 84) = 35.86$, $P< 0.0001$, sex: $F (1, 84) = 1.75$, $P= 0.18$, interaction: $F (2, 84) = 0.95$, $P= 0.39$. Post-hoc. CTL vs. LB: $P <0.0001$, LBT vs. LB: $P <0.0001$, CTL vs. LBT: $P= 0.44$. **H**. Reversal learning (probe trial) time in target zone. Rearing $F (2, 84) = 50.20$ $P<0.0001$, sex: $F (1, 84) = 1.047$ $P=0.30$, interaction $F (2, 84) = 1.536$ $P=0.22$. Post-hoc Sidak. CTL-LB $P <0.0001$, LBT-LB $P <0.0001$, CTL-LBT $P= 0.2607$. **N**. Schematic illustration of maze during reversal learning. CTL males n=18, CTL females n= 18, LB males n= 18, LB females n=18, LBT males n=10, LBT females n=10. From 7-9 different litters per group.

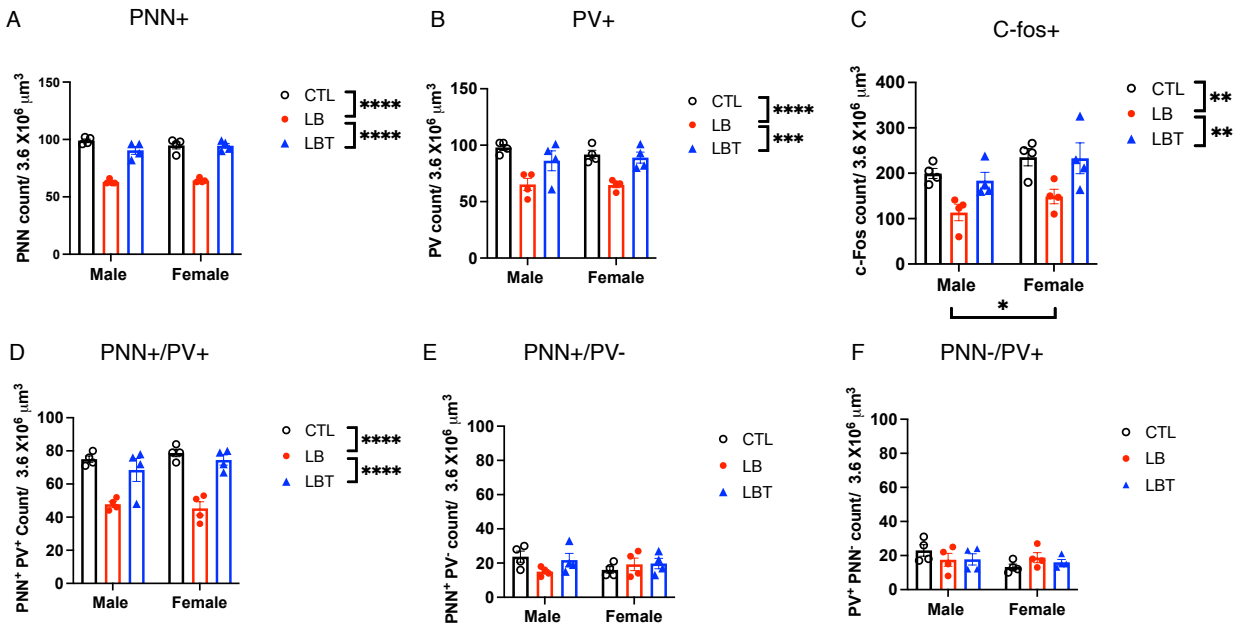

Fig S3. Effects of Rearing and Sex on PNN Formation in the OFC. This is the same data shown in Figure 2 except that outcomes in males and females are shown separately here. Postnatal Enrichment Mitigates Deficits in PNN Formation and Neuronal activation in the OFC of LB Mice **A**. PNN+ cell density. ANOVA, rearing: F (2,18) = 135.3, P< 0.0001, sex: F (1,18) = 0.034, P=0.85, interaction: F (2,18) = 1.83, P= 0.19. Post-hoc, CTL vs. LB: P< 0.0001, LBT vs. LB: P< 0.0001, CTL vs. LBT: P= 0.17. **B**. PV+ cell density. ANOVA, rearing: F (2,18) = 18.55, P< 0.0001, sex: F (1,18) = 0.10, P= 0.75, interaction: F (2,18) = 0.39, P= 0.67. Post-hoc, CTL vs. LB: P< 0.0001, LBT vs. LB: P= 0.0009, CTL vs. LBT: P= 0.35. **C**. c-fos+ cell density. ANOVA, rearing: F (2,18) = 10.54, P= 0.0009, sex: F (1,18) = 5.65, P= 0.029, interaction: F (2,18) = 0.074, P= 0.93. Post-hoc, CTL vs. LB: P= 0.0017, LBT vs. LB: P= 0.0045, CTL vs. LBT: P= 0.96. **D**. PNN+PV+ cell density. ANOVA, rearing: F (2,18) = 36.65, P< 0.0001, sex: F (1,18) = 0.61, P= 0.44, interaction: F (2,18) = 0.67, P= 0.52. Post-hoc, CTL vs. LB: P< 0.0001, LBT vs. LB: P< 0.0001, CTL vs. LBT: P= 0.35. **E**. PNN+PV- cell density. ANOVA, rearing: F (2,18) = 0.79, P= 0.46, sex: F (1,18) = 0.56, P= 0.46, interaction: F (2,18) = 2.01, P= 0.16. **F**. PNN-PV+ cell density. ANOVA, rearing: F (2,18) = 0.12, P= 0.88, sex: F (1,18) = 2.05, P= 0.17, interaction: F (2,18) = 1.89, P= 0.18. N=4 per rearing and sex group.

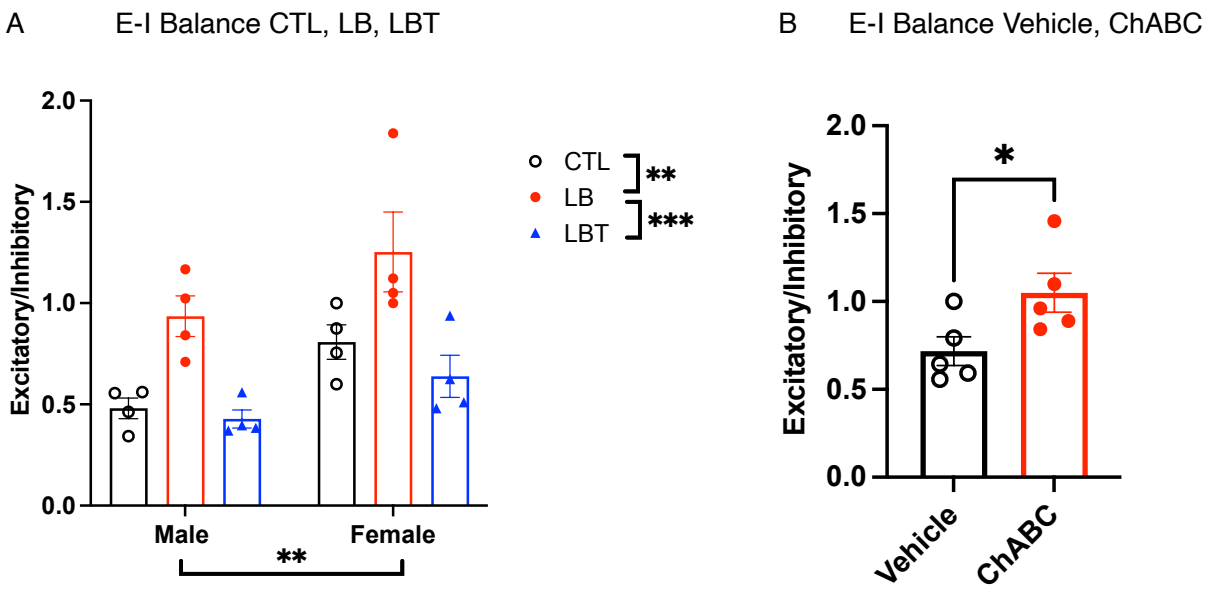

Fig S4. Effects of Rearing and PNN Degradation on the Ratio Between Excitatory and Inhibitory Synapses in the OFC. A. Postnatal enrichment normalizes E-I balance in the OFC, rearing: F (2, 18) = 14.78, P=0.0002, sex: F (1, 18) = 10.21, P=0.0050, interaction: F (2, 18) = 0.17, P= 0.84. Post-hoc Tukey's-HSD: CTL vs. LB: P= 0.0018, LBT vs. LB: P= 0.0002, CTL vs. LBT: P= 0.58. **B**. PNN degradation in the OFC increases E-I balance to levels observed in LB mice, t(8)= 2.42, P= 0.042.

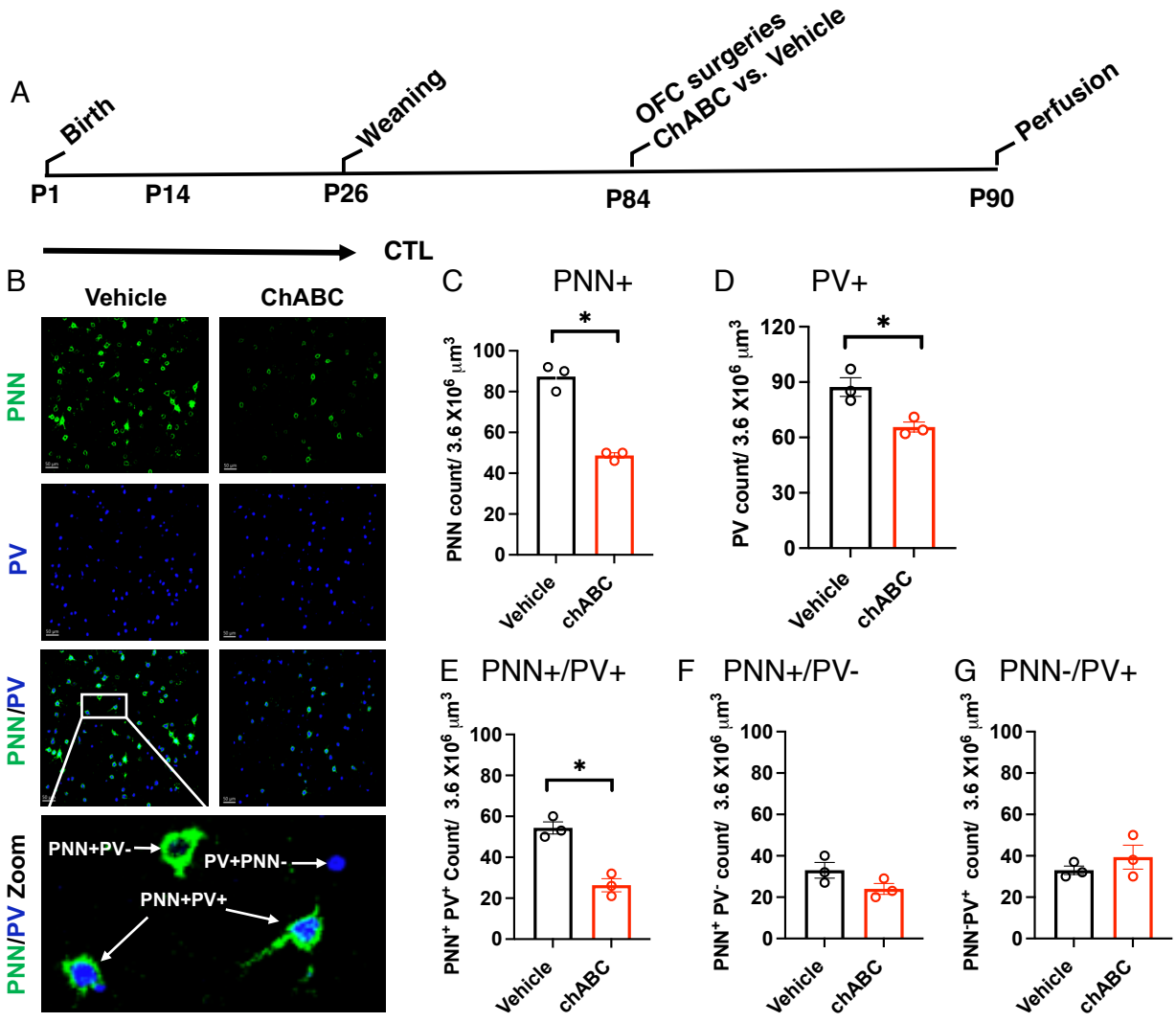

Fig S5. ChABC Treatment Reduces PNN+PV+ Cell Density in the OFC. A. Three adult Balb/cByj were administered ChABC into the right hemisphere and vehicle into the left hemisphere. Mice were sacrificed 7-days later to quantify levels of PNN+, PV+, PNN+PV+, PNN+PV-, and PNN-PV+ cells in the OFC (**B-G**). ChABC reduced the densities of PNN+ cells (**C**, t(2)= 8.29, P= 0.014), PV+ cells (**D**, t(2)= 7.31, P= 0.018) and PNN+PV+ cells (**E**, (2)= 7.39, P= 0.018), but did not alter the densities of PNN+PV- cells (**F**, t(2)= 3.58, P= 0.07) or PNN-PV+ cells (**G**, t(2)= 0.91, P= 0.45). Paired student-t-tests C-G.